COLLISIONS OF SINGLE AND MULTIPLE DROPS ONTO SOLID WALLS

D. Vadillo[1], E. Canot[2], B. Lopez[3] and A. Soucemarianadin[1]

[1]Laboratoire des Ecoulements Géophysiques et Industriels (LEGI)
B.P. 53, 38041 Grenoble Cedex 9 France
[2]IRISA, Campus de Beaulieu, 35042 Rennes Cedex, France
[3]Ardeje, 4 rue Georges Auric, 26 000 Valence, France

Abstract

This paper describes both experimental and numerical results regarding the impact of single and multiple drops onto solid walls. The experimental methods used are based on high-speed cinematography and specific phase controlled ultra short snap shots of the impact process. The advantages and drawbacks of each method and their relevance for capturing the whole impact process are discussed. Using these set-ups, we first study the case of a single drop impacting the solid substrate with a finite velocity with the rate of spreading driven by the inertia of the drop and slowed by the viscous and surface tension effects. We then model the drop impact transients using successively the variational principle and the Boundary Element Method (BEM) which allow to obtain the diameters, heights and transient profiles of the spreading drop. Comparisons between experimental and numerical results show quite fair agreement. Finally, we consider the collision of two drops focusing on the case of a drop landing on top of an other initially at rest. The preliminary experiments performed at low velocities show that after coalescence of the two drops, the swelling behavior of the liquid mass is very much alike to the case of a single drop. These results may lead to a simplified modeling of the collision of two drops for some practical situations.

1. Introduction

A large number of engineering applications are concerned with drop impact. Some of these include nuclear reactor cooling where heat transfer is affected by the drop dynamics upon impact of the drop with a solid surface, or the deleterious effect of high velocity rain drops on solid structures and on soils. Detailed knowledge of droplet impingement on solid materials is also critical for the overall process development and advancement of engineering operations such as spray cooling and/or spray coating.

The work, which is presented here, is connected in many aspects to ink-jet printing where drop impact onto solid surfaces is an ubiquitous phenomenon. The fluid flow associated with impinging drops is rather complicated because of the extreme deformation of the droplet surface occurring within very short time scales and is not really understood in detail. In the case of low impact velocities, the spreading phenomenon is probably controlled by the surface tension. When impact velocities become important, it has been shown by Rein [1] that compressibility effects play a major role. More recently Mundo *et al.* [2] have reviewed in detail the droplet wall collision problem from an experimental point of view.

The emphasis here is first on the characterization of phenomena related to low speed impacts of a single drop onto a variety of solid surfaces. At first, experimental results of the collision and deformation dynamics of a single droplet impacting on targets of glass, teflon and various grades of paper are obtained. Through these experiments we investigate not only the effects of dynamic impact conditions but also the wetting effects by detailing drop velocity, shape and size at various steps of the spreading phase [3]. We then simulate numerically the impact of single drops using models based on the variational principle [3, 5] and on the boundary element method [6, 7] and we indicate the work which still needs to be done for improving the agreement with experimental results.

Finally this study considers the fate of an incoming droplet impinging on an other which is under steady state on the substrate. This situation happens quite often in ink-jet printing where a variety of drop onto drop impacts (direct hit, partial hit, miss-hit) can be observed [8].

We consider here an axisymmetric situation with the second drop landing onto the first one which is at rest [9]. The transient interaction phenomena between the two drops are then examined in detail and comparisons with the case of a single drop are given.

2. Impact of a single drop

In this section we first describe briefly the experimental devices and detail the single droplet experiments and modeling. We will limit the discussion in this case to impacts of water drops on dry surfaces since wetted surfaces may present a host of other peculiarities as discussed by Cossali *et al.* [10] and Rioboo *et al.* [11].

2. 1. Device

The experimental set-up used comprises as ejector a syringe pump with a needle at the end and is used as a large drop generator. The device also includes a comprehensive set of built-in electronics, optical and mechanical hardware which allows taking very high magnification computer controlled photographs at different times and at different locations. We have demonstrated elsewhere [3] that the collision behavior of a single droplet is essentially controlled by the Weber and Reynolds numbers. This allows to perform experiments with scaled-up prototypes of print-heads as we have done already for drop ejection [12].

Depending on the experiment which needs to be performed, either a fast imaging camera or ordinary CCD cameras are used. The frame grabber acquires images with adjustable magnification, according to the target object. The electronic stroboscopic illumination control includes different types of illumination sources. Our electronic device allows us to deliver regularly spaced flashes of 100 ns. This allows to capture images which do not present too much blur. The apparatus is also capable of providing pseudo-cinematography movies of the entire drop impact process thanks to the fact that the phase locking is accurately controlled by computer. Further details on the design and performance of the electronic system can be found elsewhere [3, 13].

2. 2. Experiments

Figures 1a and 1b below give the evolution of a water drop of diameter 2.4 mm spreading on two different substrates. The photographs are averaged over many individual events at the same phase and the inserts indicate the time given in ms. The picture on the left hand side corresponds to a hydrophilic substrate with an equilibrium angle of 35°. The photographs on the right show the drop transients on a more hydrophobic substrate with an equilibrium angle of 70°.

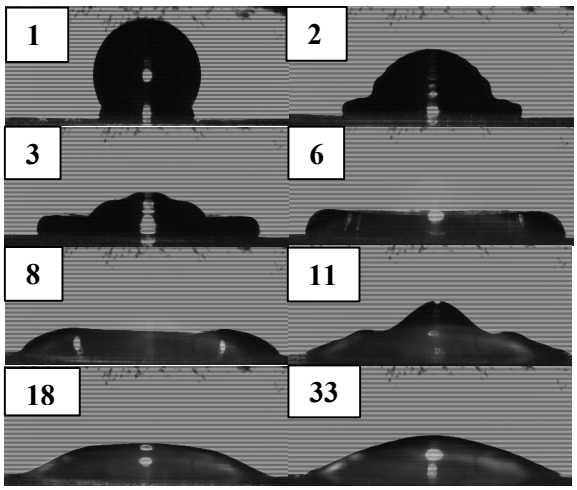

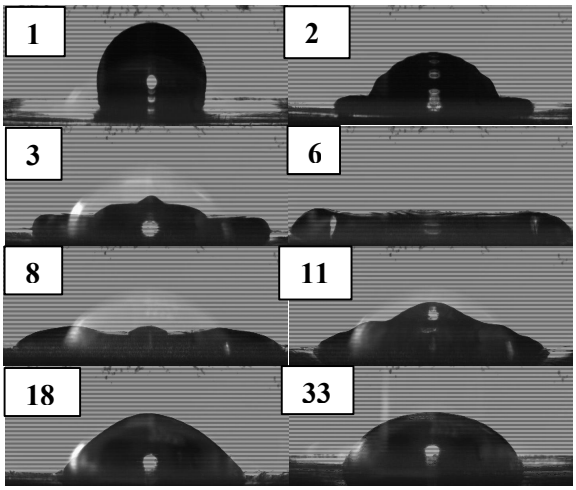

Figures 1a and 1b: Snap shots of a spreading water drop on substrates of different wetting behavior

The characteristic time for the process can be taken as D/Uo where D is the diameter and Uo the velocity of the impinging drop which in this case is equal to 1 m/s. The morphology of the drops on both substrates is almost similar with small differences becoming noticeable for the peaks of the spreading drops at 3 and at 8 ms. Real differences between figures 1a and 1b only appear when the elapsed time is more or less equal to 18 ms when the drop shape is close to equilibrium.

We plot below on figure 2 the diameter and the height of the spreading drop versus time for the hydrophobic substrate.

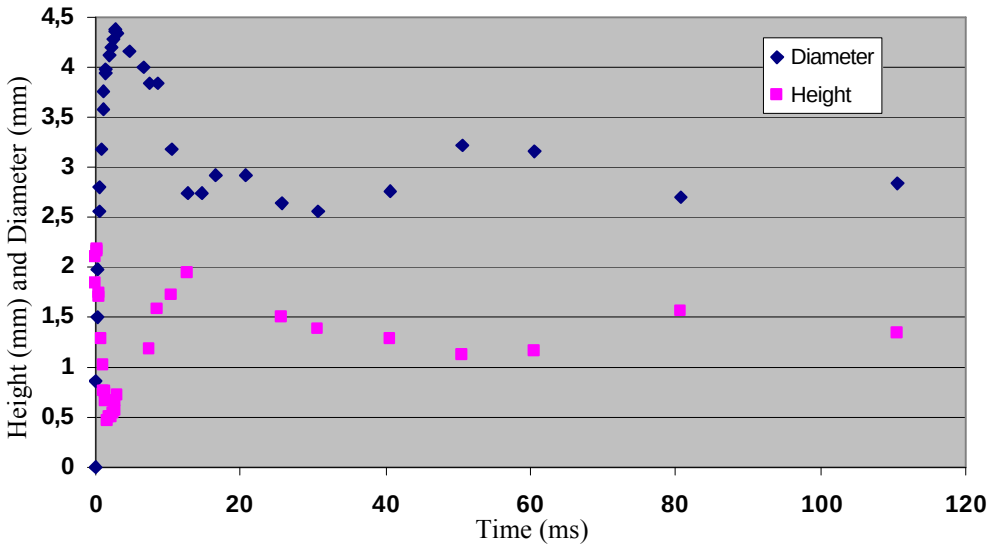

Figure 2: Transient diameter and height of the spreading drop

When the drop touches down the substrate, there is only a contact point so the diameter can be considered to be very small whilst the initial height is equal to the diameter. As expected, the largest diameter which extends from around 2 ms to almost 7 ms, (1 to 3 times the characteristic time), coincides with the lowest value for the height. The relationships between diameter, height and time cannot be defined by single power laws for the whole process which indicates that different physical mechanisms are at work with each one having its own time domain.

We have chosen to represent here the behavior for the most hydrophobic substrate because in this case an oscillation sets in at around 16 ms and is most clearly visible for the evolution of the height versus time (Fig. 2). In the case of more hydrophilic surfaces this oscillation is less pronounced or even absent as in the case of surfaces with very low equilibrium angles (smaller than 10°).

2. 3. Modeling of single drop impact

Besides the maximum value of the spreading, it is useful to have a simple model representing the drop impact transients. Indeed, the oscillation of the droplet consists of the inertial spreading of the droplet until it reaches its maximum diameter and subsequent oscillatory motions of recoiling and weak re-spreading.

The first approach to model the dynamics of single drop impact is to utilize the variational principle rather than the full Navier-Stokes equations. This method is an approximate solution of the problem in which one has to assume a specified geometry (cylinder or truncated sphere) as shown below for performing the calculations. These geometries present the advantage of relating simply the height and the diameter.

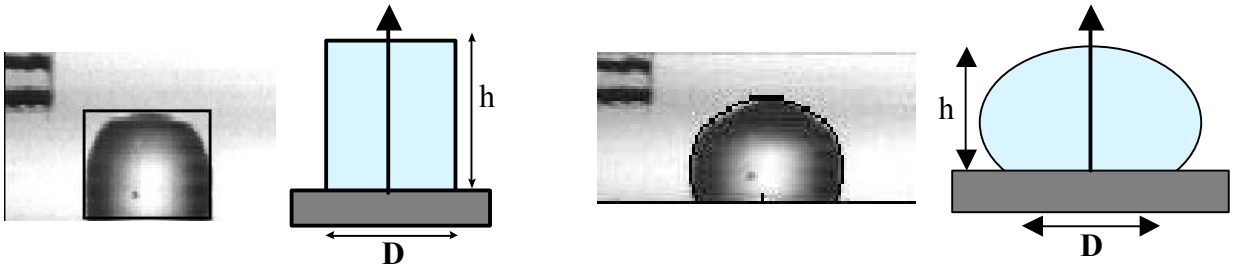

Figure 3a and 3b: Possible configurations for application of the variational method

We have shown previously [3] that the truncated sphere geometry follows more closely the actual shape of the drop all along the spreading process. For the sake of conciseness we shall only consider this geometry here. Assuming the same velocity profiles and adopting the procedure given in [4] and taking the viscous dissipation as proposed by Kim and Chun [5], a differential equation is derived for determining the drop height as a function of time during contact.

$$A(h)h''-B(h)h'^2+C(h)h'+D(h) = 0 \qquad (1)$$

where h is the drop height, the primes and double primes indicate first and second derivatives of height with respect to time and the other coefficients are some polynomial equations depending on characteristics of the fluid and the substrate.

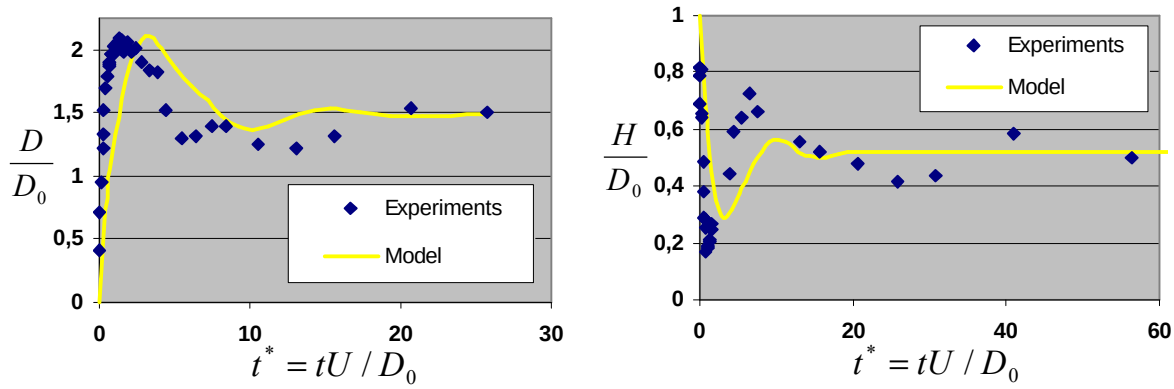

Figure 4a and 4b: Comparison between experiments and the variational model

We plot above in figures 4a and 4b the dimensionless diameter (D/Do) and height (H/Do) versus dimensionless time (Ut/Do). The viscous dissipation function is optimized so as to have agreement between the peak of the model and the actual data for say the diameter for example. All other computations are performed without further adjustments. The comparison is quite good given the uncertainty in the measurement both in the measurement of critical experimental parameters such as the wetting angle and the crude assumptions which have been made for the velocity profiles for example. Moreover this model is able to reflect quite well the observed oscillations.

One can also refer to [3] for a detailed study of various experimental situations where the above model is used by involving the Froude, Weber and Reynolds dimensionless numbers with values characteristic of ink-jet printing :

$$Fr=\frac{U^2}{gD} \qquad We=\frac{\rho U^2 D}{\sigma} \qquad Re=\frac{\rho UD}{\mu} \qquad (2)$$

g is the acceleration, U is the initial impact speed, D is the initial droplet diameter, ρ the density, μ the viscosity and σ the surface tension of the fluid.

The second approach we have used to model the single drop impact is by using the Boundary Element Method (BEM) which has the advantage of getting rid of any assumption about the shape of the spreading drop. We begin by considering the irrotational flow of an incompressible viscous liquid generated by the spreading of the liquid droplet. The initial condition of the axisymmetric configuration is that the droplet has a spherical shape already in contact with the solid boundary; moreover, the contact angle is such that the contact line velocity (which depends on contact angle) matches the geometrical speed of the interface at the point of contact.

At any time, the liquid flow can be described by a scalar potential, φ, which verifies a Laplace equation. The solid plane is a non porous boundary. Moreover the free surface is considered as a material. The dynamic boundary condition on the free surface is derived from the transient Bernoulli's equation :

$$\frac{Dj}{Dt} = \frac{1}{2}\mathbf{v}^2 + \frac{1}{We}k - \frac{2}{\mathrm{Re}}\frac{\partial^2 j}{\partial n^2} - \frac{1}{Fr}z + p_{drainage} \qquad (3)$$

The RHS of the previous equation shows inertia, surface tension, normal viscous and gravity forces. Normal viscous effects act only at the interface but induce a bulk viscous dissipation. The last term in the RHS is due to the introduction of a simple drainage model as given by El Hammoumi *et al*. [14]. Finally, dynamic contact angle behaviour is introduced via external measurement of contact angles versus spreading velocity.

The boundary value problem described in our equations can be transformed by applying the Green's second identity to the velocity potential φ, leading to an integral equation which is solved via the classical following approach, mixing Eulerian and Lagrangian formulations as described in Georgescu *et al.* [7]. The problem can be split into two and solved as follows:

a) Eulerian part: the Laplace equation is solved by a BEM solver in relation to the boundary conditions: a Dirichlet condition for the droplet interface, a Neumann condition for the solid boundary.

b) Lagrangian part: equation (3) is solved in order to update both the position of the liquid interface and the value of the velocity potential. For this time-stepping procedure, a fourth-order explicit Runge-Kutta algorithm is involved.

The boundary of the computational domain is described by a number of elements defined by nodal points. For each element, both the boundary geometry and the field functions are mapped on a low-degree polynomial basis. The integral equations thus reduce to a set of linear equations with the unknown ∂φ/∂n on the liquid interface and the unknown φ? on the rigid boundary. The set of equations is then solved by an LU decomposition method. Useful materials for this classical direct approach can be found in Brebbia *et al*. [6]. In our particular case however, the boundary geometry is approximated by cubic splines and we use linear polynomial approximation for the field functions.

When dealing with non-linear free-surface flows in a mixed Eulerian-Lagrangian formulation, the instability of the free-surface node position arises as an important problem. In order to reduce or remove this instability, a linear stability analysis based on the normal modes of a free-surface perturbation is used, providing a stability criterion for our temporal scheme as detailed by Canot [15].

We give below in figure 5 the snapshots as obtained with the BEM model for dimensionsionless numbers defined above. For these first simulations, we take the initial contact angle to be 160° and the angle at equilibrium to be 90°. One can note on this figure that the simulations predict an accumulation of mass on the extremities. More detailed comparisons with our experiments are on-going and will be reported.

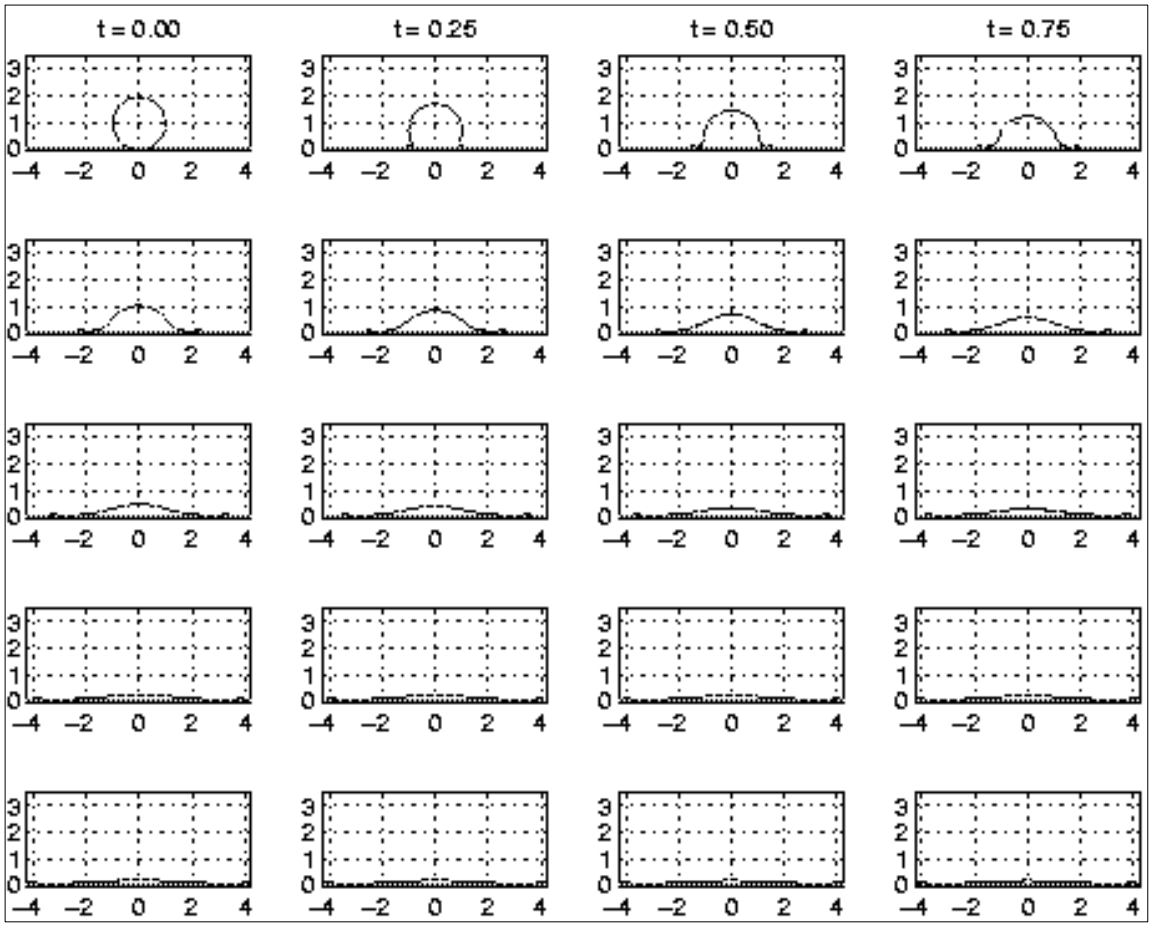

Figure 5 : Evolution of the spreading droplet versus time
Case : Fr = 5.10^4, We = 100, Re = 200

3. Multiple drop collision

Range and Feuillebois [16] recently pointed out that all works about impact can be classified into two groups: impact on dry surfaces or impact into liquid pools where the pool can be either deep or shallow. During the past few years significant progress in the understanding of the impact of a single drop onto a liquid film of uniform thickness has been made. Indeed on this topic, work with sound theoretical basis [17] was followed by extensive experimental measurements aimed at defining splash morphology [10]. Some time later, Rieber and Frohn [18] published large numerical simulations of the disintegration of the splashing lamellae and finally generalization of the theory, with inclusion of the viscosity, has been reported very recently and this enables to describe various situations [19].

On the other hand, the above literature is not directly related to our applications since droplet splashing and disintegration do very seldom occur for the case of small impact energy such as ink-jet printing and most importantly single droplet tests onto a liquid film do not consider of course the interaction effects between drops. For that purpose, we have conducted our own set of preliminary experiments with the following procedure. The first drop impinges onto the solid and reaches steady state, after some time, the second incoming drop then impacts the first in manner more or less axisymmetric because it is quite difficult to perform it correctly. The off-centered collision of drops will be considered later in order to cover the full range of possibilities of ink-jet printing [8]. The multiple drop collision tests are all conducted with a drop size of 2.4 mm and at a velocity at 1 m/s for easy comparisons with the case of a single drop on a dry substrate. The observations are performed as previously and a set of snapshots giving the multi-drop behavior is shown in figure 6. The inserts on the photographs show the time in ms and give the definitions of liquid diameter (D) and height (H).

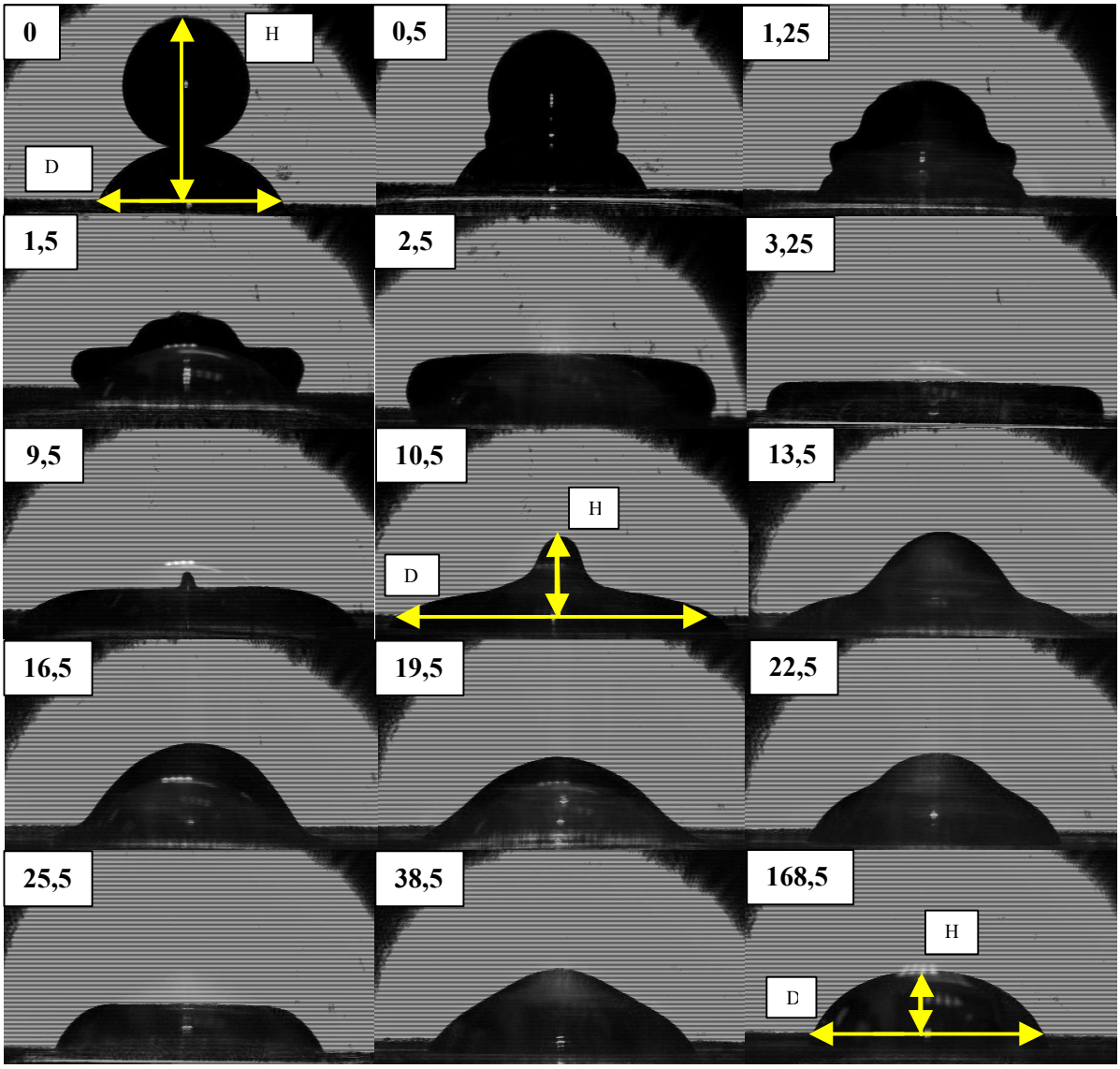

Figure 6: Collision behavior of two droplets

It can be noted from the photographs that there is no variation of the contact line before the second drop has completely immersed in the first one. This happens at about 1.5 ms and then only the liquid mass begins to swell. Figures 7a and 7 b show the evolution versus time of the diameter and height for the two drop collision together with the same data for single drop for the sake of comparison.

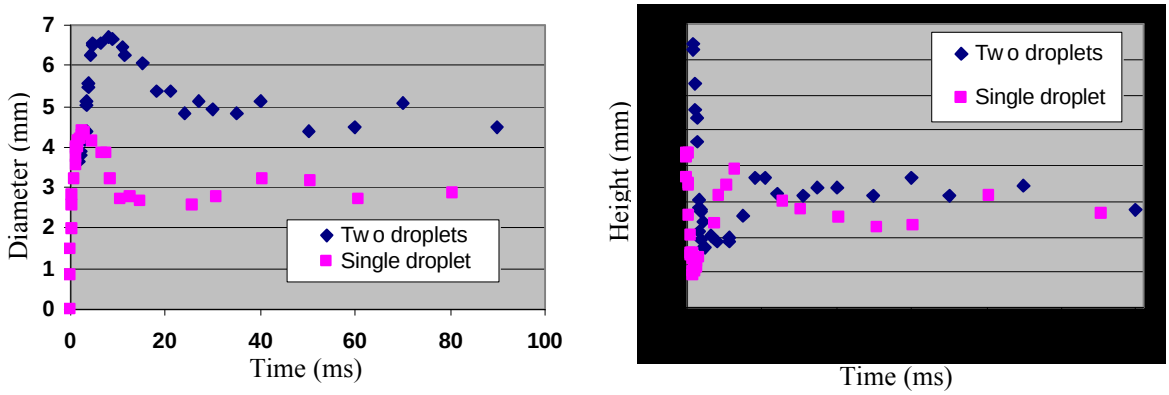

Figure 7 a and 7b: Transient diameter and height for the multi-drop impact

As shown above, the delay in the movement of the contact line for the multiple drop experiments is followed by a very steep increase in the diameter. The oscillations which are observed for the diameter are more damped than the case of the single drop and the period is slightly larger with these observations also applying for the height. Our results are quite similar to those reported by Fujimoto *et al*. [9] for their lowest velocity although we note a sharp minimum in the height which does not appear in their experiments. This may be due to the wetting behavior of the solid wall itself. More experiments need to be carried in order to ascertain the role of the parameters and to define proper dimensionless quantities.

4. Conclusions

In this paper, results concerning experiments and simulations of single drop impacts on a variety of surfaces are presented and the effect of some important physical parameters discussed. It is shown that the measurements resolve quite accurately spatial and temporal scales in the micrometers and microseconds range. Two different models are used to calculate the transient diameters and heights together with the changes in surface topology during the impact process. The results obtained compare fairly well with our experiments performed for different situations. Finally low velocity axisymmetric drop onto drop collisions show that the incoming is first absorbed into the static drop before any significant variation of the contact line.

Acknowledgments

One of the authors (A.S) is indebted to the French Ministry of Research (MRNT) for partial financial support of this work through project Σ ! 2911 PRODIJ.

References

[1] Rein M. 1993 *Fluid Dynamics Res*., vol. **12**, 61-93.
[2] Mundo CHR, Sommerfeld M and Tropea C. 1995 *Int. J. of Multiphase Flow*, vol. **21**, 151-173.
[3] Desie G, Allaman S, Vadillo D and Soucemarianadin A 2003 submitted to *J. of Imaging Sci. and Technol*.
[4] Bechtel S.E., Bogy D.B. and Talke F.E 1981 *IBM J. Res. Dev*., vol. **25**, 963-
[5] Kim H.Y, and Chun J.H. 2001 *Physics of Fluids*, vol. **13**, 643-659.
[6] Brebbia C.A., Telles J.C.F. and Wrobel L.C. 1984 *Boundary Element Techniques. Theory and Applications in Engineering*. Springer-Verlag.
[7] Georgescu S.C., Achard J.L. and Canot E. 2002 *Eur. J. Mech., B/Fluids*, vol. **21**, 265-280.
[8] Oliver J.F. 1984 *Tappi Journal*, vol. **10**, 90-94.
[9] Fujimoto H., Tomoyuki O., Takuda H. and Hatta N. 2001 *Int. J. of Multiphase Flow*, vol. **27**, 1227-1245.
[10] Cossali, G.E., Coghe A. and Marengo M. 1997 *Exp. in Fluids*, vol. **22**, 463-472.
[11] Rioboo R., Marengo M., Cossali G.E. and Tropea C. 2000 *Proc. ILASS-Europe 2000*, **VII**.11.1-11.5.
[12] Lopez B., Kalaaji A., Soucemarianadin A., and Attané P. 2000 *Proc.16th Intl. Non-Impact Printing Conf.*, 65-72.
[13] Lopez B., Vadillo D., Pierron P., and Soucemarianadin A., 2002 *Proc.18th Intl. Non-Impact Printing Conf.*, 170-175.
[14] El Hammoumi M., Canot E., Davoust L., Lachkar D., 2003 *Theo. Comp. Fluid Dyn*., (under press).
[15] Canot É.,1999 *Proc. of the Int. Conf. On Boundary Element Techniques*, 321-330.
[16] Range K. and Feuillebois F., 1998 *J. of Colloid and Interf. Sci*., vol. **203**, 16-30.
[17] Yarin A.L., and Weiss D.A., 1995 *J. of Fluid Mech*. vol. **283**, 141-173.
[18] Rieber M. and Frohn A., 1999 *Intl J. of Heat and Fluid Flow* vol. **20**, 455-461.
[19] Roisman I.V. and Tropea C., 2003. *J. of Fluid Mech.* vol. 472, 373-397.